TMS2014 Annual Meeting Supplemental Proceedings
TMS (The Minerals, Metals & Materials Society), 2014

TiO_2 NANOTUBES FILLED WITH $NiFe_2O_4$ QUANTUM DOTS OR Ni-Fe NANOALLOY: SYNTHESIS AND APPLICATIONS

M. Y. Mohassab-Ahmed[1], A. F. Moustafa[2], A. A. Farghali[2], H. Y. Sohn[1], and M. H. Khedr[2]

[1] Metallurgical Engineering Department, University of Utah, Salt Lake City, UT 84112, USA
[2] Chemistry Department, Beni-Sueif University, Beni-Sueif 62111, Egypt

Keywords: TiO_2, Nanotubes, Quantum Dots, Gas Sensing, Photdegradation

Abstract

Titania nanotubes (TiO_2-NTs) were prepared from anatase TiO_2 nanopowder with a crystallite size of 90 nm by a hydrothermal method followed by ion exchange. The obtained TiO_2-NTs were filled with $NiFe_2O_4$ quantum dots (QDs) and subjected to hydrogen at 600°C to produce TiO_2-NTs filled with Ni-Fe nanoalloy. Filling TiO_2-NTs with $NiFe_2O_4$ quantum dots shifted the absorption edge of the nanotubes to the visible region, narrowing the band gap of TiO_x-NTs. The modified TiO_2-NTs were investigated for the degradation of toxic dyes for water treatment. These TiO_2NTs offered high degrees of photodegradation of the organic dyes with high visible light activity. They also were a promising corrosion inhibitor. The electrical conductivity-temperature dependences of empty anatase TiO_2-NTs, anatase TiO_2-NTs filled with $NiFe_2O_4$ QDs, anatase TiO_2-NTs filled with Ni-Fe nanoalloy and $NiFe_2O_4$ compact disks were measured in the temperature range 25-850 °C. The modified TiO_2-NTs were also tested for CO_2 sensing.

Introduction

TiO_2 is a promising photocatalyst due to its inherent destructive capabilities towards organic dyes. The photodegradation of organic dyes on the surface of TiO_2 can be carried out under ambient conditions (atmospheric oxygen is used as oxidant) and may lead to complete mineralization of organic carbon into CO_2 [1]. TiO_2 in the form of nanotubes (TiO_2-NTs) is expected to have some improved properties for photocatalytic applications compared with colloidal or other forms of titania [2]. The tubular structure, large surface-to-volume ratio, and high sedimentation rate are distinct properties of TiO_2-NTs [3]. As a result, TiO_2-NTs are more suitable as a catalyst or catalyst support for the heterogeneous catalytic reactions and other applications [3]. Also, TiO_2 has been used as protective coatings against corrosion [4]. In addition, the anatase form of TiO_2 has been examined for the sensing of CO and CH_4 at temperatures of 873 K [5]. Despite the aforementioned properties, TiO_2-NTs still suffer from the problems of high e^- and h^+ recombination rate [6] and high energy gap (3.6 eV) [7]. Other challenge for using TiO_2-NTs is the low quantum yield of TiO_2-based photocatalysis. To overcome these problems, many efforts have been made to modify TiO_2-NTs. This work, for the first time, investigates TiO_2-NTs modified with $NiFe_2O_4$ or NiFe nanoalloy for photocatalysis, CO_2 sensing, corrosion inhibition, and heavy metal adsorption applications.

In the present work, TiO_2-based NTs were investigated in terms of their visible-light catalytic activity for water treatment applications. Titanate NTs, anatase TiO_2-NTs, anatase TiO_2-NTs filled with $NiFe_2O_4$-QDs, and anatase TiO_2-NTs filled with Ni-Fe nanoalloy and $NiFe_2O_4$ were examined for photodegradation of some organic dyes. In addition, a degradation mechanism of Bromopyrogallol red (Bp red) dye was proposed. Kinetic analysis of the degradation process on the surfaces on the new catalysts under visible light and in dark was conducted.

Experimental details

Synthesis

Anatase-phase TiO_2-NTs was prepared by dispersing 5 gm of TiO_2 powder in 150 mL of 10 M NaOH and stirring for 15 min. The dispersion was then transferred to a Teflon-lined autoclave and was kept at $150^{\circ}C$ for 124 hours. A white precipitate ($Na_2Ti_3O_7$) was obtained. This precipitate was washed first with HCl to neutralize the excess NaOH and replace Na^+ to form $H_2Ti_3O_7$. Anatase-phase TiO_2-NTs was then obtained by dehydration at 500 °C. To fill TiO_2-NTs with $NiFe_2O_4$, an aqueous solution of $Ni(NO_3)_2$ and $Fe(NO_3)_3$ with a molar ratio of 1:2 was mixed with the TiO_2-NTs and stirred with a magnetic stirrer for 30 min under vacuum. The mixture was then kept overnight, filtered and washed with distilled water. The precipitate was transferred to a beaker containing 50 mL of 1 M NaOH and stirred for 30 min at $60^{\circ}C$, filtered, washed well with distilled water, dried at $100^{\circ}C$ for 1 hour, and finally fired at $600^{\circ}C$ for 3 hours [8]. $NiFe_2O_4$ was previously prepared by the self-flash combustion method described in details elsewhere [9]. In this method, aqueous solutions of $Ni(NO_3)_2$ and $Fe(NO_3)_3$ with molar ratio of 1:2 were mixed and then dried at 100°C for 24 hours. Then the powder was heated vigorously on a hot plate to ensure the complete decomposition of nitrate. Finally, the obtained powder was heated at 600 °C for 3 hours to form $NiFe_2O_4$ with the crystal size ranging from 9 to 12 nm [8]. Ni–Fe nanoalloy was prepared by the reduction of the synthesized $NiFe_2O_4$ by H_2 gas at 600 °C to produce Ni–Fe nanoalloy with particle size in the range of 8–10 nm [10]. The same procedure was adopted to prepare TiO_2-NTs filled with Ni–Fe nanoalloy where $NiFe_2O_4$– TiO_2-NTs was reduced with H_2 at 600 °C to produce Ni-Fe with a particle size similar to that of the free nanoalloy. Phase identification and crystallite size of the prepared materials was determined by X-ray diffractometer (JSX-60P JEOL®). The morphology and particle size of the prepared materials were analyzed using transmission electron microscope (TEM-JOEL, JEM-1234®), a UV–Visible (UV–Vis) spectrometer was used to obtain the absorption spectra of the samples, and finally the surface topography was investigated by SEM.

Photocatalytic degradation

All the photocatalysts (titanate NTs, anatase TiO_2-NTs, anatase TiO_2-NTs filled with $NiFe_2O_4$-QDs, and anatase TiO_2-NTs filled with Ni-Fe nanoalloy and $NiFe_2O_4$) were examined for degradation of several toxic organic dyes [Bromopyrogallol red (Bp red), Toluidine Blue (TB) and Methylene Blue (MB)]. A photocatalyst of 0.2 g was added to 100 ml of 1×10^{-7} M of the tested dye.

Gas Sensing

Compact disks of the synthesized nanomaterials were mounted between two stainless steel electrodes of in an electrical conductivity cell and held tightly with springs. The cell was then placed inside a vertical tube furnace set at 350°C. The vertical furnace containing the cell was implemented in a system that consisted mainly of two units: (1) gas purification and (2) gas sensing unit. The purification unit consisted of copper gauze heated to 550°C in a tube furnace to remove oxygen from the gas stream. Silica gel and anhydrous calcium chloride towers and (C) respectively were used for drying the gas. Moreover, to remove any traces of CO_2 expected to be contaminated N_2 gas was allowed to pass through a Soda lime tower. The gas sensing unit consisted of the electrical cell installed in the vertical tube furnace and computerized Avometer (H) (BK precision Avometer model 390A). The sensor was allowed to stabilize at the operating temperature for 30 min under N_2 flow of 1000 sccm/min. The tested gas (CO_2) was adjusted at 2, 4, 6 sccm at the operating temperature in the presence of N_2 gas to create the necessary test gas atmosphere. The total resistance of the samples compacts was measured by the computerized Avometer.

Corrosion Resistance Measurements

Equal weights of free Ni-Fe nanoalloy and Ni-Fe nanoalloy coated with TiO_2-NTs were compressed into disks using a cylindrical mold of 1 cm inner diameter using an applying pressure 250 kg/m^2. The disks were then heated at 110°C for about 2 hours and weighed before immersion in 0.5 M HCl solution for 20, 40, 60 and 150 minutes at different temperatures ranged from 25°C to 75°C. The corrosion rate was calculated using the following equation [8]:

$$R = \frac{(W_o - W)}{A \times t} \qquad (1)$$

where W_o and W are the weight of the sample before and after immersion in the HCl solution, respectively. A is the surface area of the sample and t is the immersion time.

The inhibition efficiency (*%P*) of TiO_2-NTs at different temperatures and time were calculated using the following equation:

$$\%P = 100 \times \left(1 - \frac{W}{W_o}\right) \qquad (2)$$

where *%P* is the inhibition efficiency, W_o and W are the weight loss per min. in the HCl solution respectively.

Results

Synthesis

Figure 1 shows a TEM image of the obtained TiOx-NTs the nanotubes prepared at 150 °C for 124 hours were of good quality, layered structure, good crystallinity and complete rolling. The obtained nanotubes had 10 nm inner and 37 nm outer diameters. In addition, the nanotubes were hollow and open-ended. The XRD patterns for the prepared nanomaterials show different phases of titanium oxides (Ti_2O_3, Ti_4O_7, rutile TiO_2), as illustrated in Figure 2. The obtained nanotubes were found to be of low crystallinity due to their small crystal size. The first two phases were deficient in the oxygen content where the titanium valances are Ti^{+3} and $Ti^{+3.5}$, whereas in the third phase the titanium valance was Ti^{+4}. Thus, to obtain single phase TiO_2-NTs, the obtained nanotubes were fired at 500°C at a low flow rate of oxygen gas (5-7 sccm) for 2 hours. The XRD pattern in Figure 2(c) shows that the phase transformation process was complete. The different phases of titanium oxides disappeared, and a single anatase phase of TiO_2-NTs with high crystallinity was obtained.

Filling of TiO_2-NTs and their thermal stability

The tubular structure of TiO_2-NTs was preserved even after annealing at 600°C for 3 hours to form $NiFe_2O_4$-QDs. This indicates the high thermal stability of the prepared nanotubes. Figure 2(f) shows XRD patterns of highly filled TiO_2-NTs with $NiFe_2O_4$-QDs. There are only two phases, anatase phase TiO_2 and $NiFe_2O_4$, with no evidence of the presence of any other phases such as Ni, Fe or Ti oxides. Low crystallinity may be attributed to the small crystal size and high dispersion of $NiFe_2O_4$-QDs inside the nanotubes, as illustrated before [11]. Thus, it is concluded

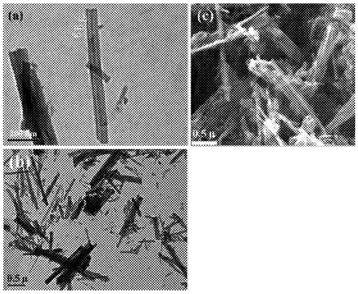

Figure 1. TEM images for TiO_2-NTs prepared at 150°C for 124 hours revealing: (a) the layered structure, (b) as-prepared of TiO_2-NTs, indicating a high yield of nanotubes, and (c) SEM image for TiO_2-NTs.

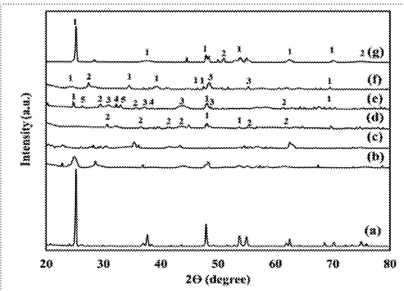

Figure 2. XRD patterns of (a) anatase TiO_2, (b) anatase TiO_2-NTs, (c) $NiFe_2O_4$, (d) anatase TiO_2-NTs filled with $NiFe_2O_4$-QDs; 1: anatase and 2: $NiFe_2O_4$, (e) partially filled TiO_2-NTs; 1: Ti_2O_3, 2: Ti_4O_7, 3: rutile TiO_2, 4: Fe_3O_4 and 5: Fe_2O_3, (f) mixed oxide; 1: Ti_2O_3, 2: Ti_4O_7 and 3: rutile TiO_2, and (g) anatase TiO_2-NTs filled with Ni-Fe nanoalloy; 1: anatase, 2: Ni-Fe.

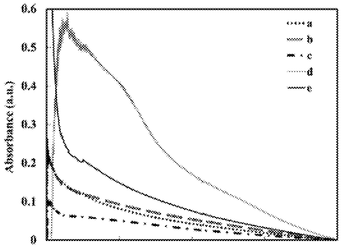

Figure 3. UV-vis absorption spectra of (a) titanate NTs, (b) anatase TiO_2-NTs, (c) $NiFe_2O_4$, (d) anatase TiO_2-NTs filled with $NiFe_2O_4$-QDs, and (e) anatase TiO_2-NTs filled with Ni-Fe.

that the new conditions of the filling process help in the transformation of other Ti oxides to a pure anatase phase of TiO_2. The oxygen deficiency was produced by the release of nitric oxide vapors during the firing step in air at 600°C for 3 hours to form $NiFe_2O_4$-QDs. Figure 3 illustrates the UV-visible absorption spectra of titanate NTs, anatase TiO_2-NTs, $NiFe_2O_4$ nanoparticles, anatase TiO_2-NTs filled with $NiFe_2O_4$-QDs, and anatase TiO_2-NTs filled with Ni-Fe nanoalloy. It was found that the annealing and filling process markedly enhanced the visible response of TiO_2-NTs. The band gap absorption edge of the samples was determined according to the following relationship [7]:

$$E_g = \frac{1240}{\lambda} \qquad (3)$$

where λ is the optical absorption threshold. The absorption edges of titanate NTs, $NiFe_2O_4$ nanoparticles, anatase TiO_2-NTs anatase TiO_2-NTs filled with Ni-Fe, and anatase TiO_2-NTs filled with $NiFe_2O_4$-QDs were, respectively, 386, 395, 396, 470 and 770 nm, which correspond to the band gap energies of 3.21, 3.14, 3.13, 2.64, and 1.61 eV, respectively. It is seen that the filling process shifted the absorbance of the TiO_2-NTs to the visible region. the band gap of the anatase-phase TiO_2-NTs filled with $NiFe_2O_4$-QDs has the lowest value because the $NiFe_2O_4$-QDs narrowed the band gap of the NTs [8]. In addition, the band gap of the as-prepared TiO_2-NTs and the TiO_2-NTs annealed at 600°C are lower than the values observed in the work done by Wang *et al.* [12]. This can be attributed to the preparation conditions, higher temperature and longer time of thermal treatment in this work (150°C for 124 h). In the present investigation, the prepared TiO_2-NTs had high thermal stability even after calcination at 600°C for 3 hours and maintained their tubular and layered structure, as illustrated in the TEM images of Figure 1.

Photocatalytic degradation

It was found that the visible light irradiation without catalyst causes the decomposition of approximately 17% of Bp red after 260 min, whereas the degradation rate increases in the presence of empty anatase TiO_2-NTs, $NiFe_2O_4$ and titanate NTs to about 79%, 85%, and 89%, respectively. About 99+% degradation of Bp red dye was observed with two catalysts: (1) anatase TiO_2 filled with Ni-Fe nanoalloy after 260 min and (2) anatase TiO_2-NTs filled with $NiFe_2O_4$-QDs after 80 min. Therefore, anatase TiO_2-NTs filled with $NiFe_2O_4$-QDs photocatalyst has high photocatalytic activity and remarkable visible light response. Based on the degradation results of Bp red, it is clear that the degradation percentage increases with decreasing narrowing the band gap due to the decrease in the energy required for generation of conduction band electrons (e^-) and valence band holes (h^+). In addition, the absorption edge of the titanium oxides NTs was found to be 386 nm, which is close to that of bulk anatase TiO_2 (385 nm). Anatase TiO_2-NTs showed a shift in the absorption edge (396 nm) compared with bulk anatase TiO_2. This shift is attributed to the phase transformation of the titanate NTs to anatase TiO_2-NTs and the crystal growth of new phases.

Gas Sensing

Figure 4 shows the response of anatase phase TiO_2-NTs as a function of different CO_2 gas concentrations at 350°C by switching from a nitrogen environment to a mixture of nitrogen and different concentration of CO_2, and then back to nitrogen. It can be seen that the response of the sensor increased with the CO_2 concentration from 2, 4 to 6 sccm at constant temperature 350°C which is a typical for semiconductor type gas sensor. For anatase phase TiO_2-NTs filled with $NiFe_2O_4$-QDs, there is an increase in the response of the sensor with increasing CO_2 concentration but with higher magnitude than that observed with the first sensor (anatase phase

TiO_2-NTs). Anatase TiO_2-NTs filled with Ni-Fe nanoalloy showed the highest response towards CO_2 gas. It was also found that the sensitivity of the three gas sensors increased with CO_2 gas concentration with the highest value for the anatase TiO_2-NTs filled with Ni-Fe nanoalloy sensor at 350°C. Sensitivity was found to increase with concentration but at high concentration the increase in sensitivity is beginning to saturate for anatase TiO_2-NTs filled with Ni-Fe nanoalloy gas sensor. The response times for empty anatase TiO_2-NTs, anatase TiO_2-NTs filled with $NiFe_2O_4$ and anatase TiO_2-NTs filled with Ni-Fe nanoalloy are 90, 120, 50 s, respectively.

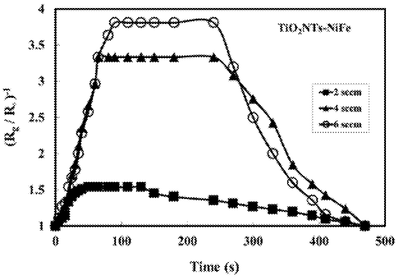

Fig. 2. Variation of resistance Rg, normalized with respect to baseline resistance, R₀, of anatase TiO_2-NTs filled with Ni-Fe with time as a result of exposure to 2, 4, and 6 sccm CO_2 gas at 350°C. The inverse of R_g/R_o was used for representing data in positive y-direction.

Corrosion Resistance

TiO_2-NTs were tested as coating material for the corrosion protection of Ni-Fe nanoalloy in a corrosive environment. The weight loss of Ni-Fe nanoalloys in a 0.5 M HCl solution with and without TiO_2-NTs coatings was measured as a function of immersion time at different temperatures (25, 50 and 75 °C). Table 1 lists the weight loss of uncoated and coated nanoalloy at different temperatures after an immersion time of 150 min. For TiO_2-NTs coated materials the obtained weight loss was found to be very small as compared to uncoated Ni-Fe alloy. It was found that the weight loss of the coated alloys was 21, 27 and 1.5 times less than that of the uncoated alloys at 25, 50 and 75 °C, respectively. It appears also that TiO_2-NTs retain their protective ability even after long immersion times. These results indicate that TiO_2-NTs could significantly depress the acid interactions with Ni-Fe nanoalloy. Thus, TiO_2-NTs could be a good corrosion inhibitor with high protective capability.

Table 1. Weight loss of free and coated Ni-Fe nanoalloy at different temperatures after an immersion time of 150 min.

Temperature (°C)	Weight loss (%)	
	Free nanoalloy	Coated nanoalloy
25	63.6	3.1
50	94.5	3.5
75	96.5	62.6

The variation of the inhibition efficiency (*%P*) with time at different temperatures was also investigated. Inhibition efficiency values were 99.3 %, 99.2 % and 87.7 % at 25, 50 and 75°C, respectively. This indicates that the TiO_2-NTs offer high inhibition efficiency even after long immersion time and at high temperatures. This could be attributed to the ceramic protective barrier formed by TiO_2-NTs, which protects the Ni-Fe nanoalloy from direct contact with the corrosive medium. Furthermore, photo-generated cathodic protection currents increase due to presence of Ni-Fe nanoalloy inside TiO_2-NTs. The Ni-Fe nanoalloy narrows the band gap of TiO_2-NTs and hence shifts its response to visible region and reduces the potential required for generation of charge carriers. The decrease of inhibition efficiency at a higher reaction temperature (75°C) could be attributed to diffusion of HCl into TiO_2-NTs, which leads to dissolution of the Ni-Fe nanoalloy. As a result, TiO_2-NTs offer promising and efficient corrosion inhibitor.

Electrical Conductivity

Figure 5 shows the DC conductivity (σ) of the samples to the temperature during a heating-cooling cycle. During cooling the conductivity retains values higher than that obtained during heating; this may be explained by the fact that the electrical conductivity of semiconductor materials is significantly affected by the oxygen vacancies and/or lattice defects within the sample [8]. In case of TiO_2-NTs filled with $NiFe_2O_4$ QDs, during cooling the samples exhibit reversible behavior. At higher temperatures the behavior is irreversible due to phase transformation and destruction of TiO_2-NTs. The overall behavior is linear-like, which may be attributed to filling $NiFe_2O_4$ with QDs. Table 2 presents the conductivity values (σ $(\Omega cm)^{-1}$) of the tested samples at 850 °C. It was found that the conductivity of empty anatase TiO_2-NTs is higher than that of TiO_2-NTs filled with $NiFe_2O_4$ QDs. This could be a result of the firing step of TiO_2-NTs at 600 °C to form $NiFe_2O_4$ DQs which might affect the defect density and hence the conductivity value. On the other hand, TiO_2-NTs filled with Ni-Fe nanoalloy. The overall behavior is irreversible. The conductivity values at 850°C are lower than those observed for empty TiO_2-NTs or TiO_2-NTs filled with $NiFe_2O_4$ QDs. This may be attributed to the reduction process carried out to produce TiO_2-NTs filled with Ni-Fe nanoalloy. This reduction is believed to affect the density of defects and the oxygen vacancies within the sample as the removal of the adsorbed and structural oxygen from TiO_2-NTs and $NiFe_2O_4$ affects the oxygen stoichiometry and consequently the conductivity of the sample.

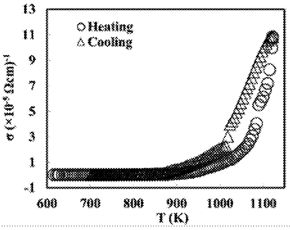

Figure 5. The conductivity of empty anatase TiO_2-NTs

Conclusions

TiO_2-NTs were prepared by a hydrothermal method followed by an ion exchange process at different times and temperatures. The NTs prepared at a 150 °C for 124 hours showed good crystallinity, high throughput and layered structures as compared with those prepared at 130 °C for 48 hours. TiO_2-NTs filled with $NiFe_2O_4$-QDs showed the highest photocatalytic activity for degradation of the tested dyes. Filling TiO_2-NTs with $NiFe_2O_4$-QDs or Ni-Fe nanoalloy was found to narrow the band gaps of TiO_2-NTs and therefore shifted the response of TiO_2-NTs to the visible light region. Anatase TiO_2-NTs filled with Ni-Fe nanoalloy showed the highest response towards CO_2 gas. The response times for empty anatase TiO_2-NTs, anatase TiO_2-NTs filled with $NiFe_2O_4$ and anatase TiO_2-NTs filled with Ni-Fe nanoalloy are 90, 120, 50 s, respectively. TiO_2-NTs offer promising and efficient corrosion inhibitor. Filling TiO_2-NTs with $NiFe_2O_4$ or Ni-Fe nanoalloys was found to change the conductivity-temperature behavior of TiO_2-NTs

References

1. I.K. Konstantinou and T.A. Albanis, "Photocatalytic Transformation of Pesticides in Aqueous Titanium Dioxide Suspensions Using Artificial and Solar Light: Intermediates and Degradation Pathways." *Appl. Catal. B-Environ.*, 42 (2003), 319-335.
2. A. Ghicov, J.M. Macak, H. Tsuchiya, J. Kunze, V. Haeublein, L. Frey, and P. Schmuki, "Ion Implantation and Annealing for an Efficient N-Doping of TiO_2 Nanotubes." *Nano Letters*, 6 (2006), 1080-1082.
3. X. Quan, S. Yang, X. Ruan, and H. Zhao, "Preparation of Titania Nanotubes and Their Environmental Applications as Electrode." *Environmental Science and Technology*, 39 (2005), 3770-3775.
4. K. Meinert, C. Uerpmann, J. Matschullat, and G. Wolf, "Corrosion and Leaching of Silver Doped Ceramic Ibad Coatings on SS 316L under Simulated Physiological Conditions." *Surface and Coatings Technology*, 103 (1998), 58-65.
5. N.O. Savage, S.A. Akbar, and P.K. Dutta, "Titanium Dioxide Based High Temperature Carbon Monoxide Selective Sensor." *Sensor. Actuat. B-Chem.*, 72 (2001), 239-248.
6. C. Wang, C. Böttcher, D.W. Bahnemann, and J.K. Dohrmann, "A Comparative Study of Nanometer Sized Fe(Iii)-Doped Tio_2 Photocatalysts: Synthesis, Characterization and Activity." *Journal of Materials Chemistry*, 13 (2003), 2322-2329.
7. N. Wang, H. Lin, J. Li, X. Yang, B. Chi, and C. Lin, "Effect of Annealing Temperature on Phase Transition and Optical Property of Titanate Nanotubes Prepared by Ion Exchange Approach." *Journal of Alloys and Compounds*, 424 (2006), 311-314.
8. M. Bahgat, A.A. Farghali, A.F. Moustafa, M.H. Khedr, and M.Y. Mohassab-Ahmed, "Electrical, Magnetic, and Corrosion Resistance Properties of TiO_2 Nanotubes Filled with $NiFe_2O_4$ Quantum Dots and Ni–Fe Nanoalloy." *Appl. Nanos*, (2012), 1-9.
9. A. Farghali, M. Khedr, and A. Moustafa, "Photocatalytic Activity and Magnetic Properties of Nanocrystallite Strontium Hexaferrite Prepared by Self-Flash Combustion." *Mater. Tech.: Advanced Perf. Mater.*, 23 (2008), 104-109.
10. J. Lee, T. Kim, J. Yu, and S. Chung, "In-Situ Alloying on Synthesis of Nanosized Ni-Fe Powder." *Nanostructured Materials*, 9 (1997), 153-156.
11. Y. Yu, H.-H. Wu, B.-L. Zhu, S.-R. Wang, W.-P. Huang, S.-H. Wu, and S.-M. Zhang, "Preparation, Characterization and Photocatalytic Activities of F-Doped TiO_2 Nanotubes." *Catalysis Letters*, 121 (2008), 165-171.
12. N. Wang, H. Lin, J. Li, X. Yang, B. Chi, and C. Lin, "Effect of Annealing Temperature on Phase Transition and Optical Property of Titanate Nanotubes Prepared by Ion Exchange Approach." *Journal of Alloys and Compounds*, 424 (2006), 311-314.